k_G as a Passive Lithological Compliance Index: Derivation from Independent Spectral Residuals and Validation across Seven Lithologies

Benjamin Gasque

Independent Researcher · SAS Food and Beer
Claouey, Lège-Cap-Ferret, 33950, France
a2m.arlac@gmail.com
ORCID: https://orcid.org/0009-0003-7018-5813

ORCID Profile: https://orcid.org/0009-0003-7018-5813
Affiliation: SAS Food and Beer, Claouey, France
Domain: Independent researcher — Passive geophysics, Archaeological seismology, Defense sensing (2 patents INPI filed March 2026)

k_G as a Passive Lithological Compliance Index: Derivation from Independent Spectral Residuals and Validation across Seven Lithologies

Running title: Passive seismic site characterization with the Gasque compliance index

Benjamin Gasque

Independent Researcher · SAS Food and Beer, Claouey, Lège-Cap-Ferret, 33950, France
a2m.arlac@gmail.com | ORCID: https://orcid.org/0009-0003-7018-5813

Abstract

We present $k_G = \pi \times f_0 / (Q \times V_s)$ as a passive lithological compliance index measurable from ambient seismic noise without drilling or active sources. The fundamental frequency f_0 is extracted from spectral residuals after subtraction of the common seismic mode (oceanic microseism), while V_s and Q are drawn from published borehole measurements. Using this three-source independent framework across nine broadband seismic stations spanning seven lithological classes — granite, ophiolite, basalt, limestone, marl, alluvium, and soft sediment — we find a near-perfect Spearman correlation between k_G and $Q \times V_s$ ($\rho = -0.941$, p = 0.0002, N = 9). The lithological ordering granite < ophiolite < basalt < limestone < marl < alluvium < sediment is recovered consistently across six spectral window lengths (5 min to 2 h), with coefficient of variation below 3% at five of nine stations. A formal independence test confirms that f_0 carries no information about $Q \times V_s$ ($\rho = -0.008$, p = 0.98), ruling out algebraic circularity. In Theban limestone, the empirically calibrated value $k_G = 23.1$ /km (Gasque, 2026; $\rho = 0.786$, p = 0.021, N = 8 tombs) exceeds the borehole-derived compliance value of 0.055 /km by a factor of 420, encoding cavity resonance amplification. We propose k_G as a single-station, equipment-agnostic site-characterization parameter complementary to V_{s30}, requiring no instrument deployment beyond existing network infrastructure. All data, methods, and results are fully reproducible from public seismic archives.

Keywords: passive seismic · lithological compliance index · seismic site characterization · quality factor Q · ambient noise · HVSR · k_G detectability · Theban limestone · FDSN open data · spectral residuals · common-mode subtraction

1. Introduction

Characterizing the mechanical properties of the shallow subsurface is a prerequisite for seismic hazard assessment, archaeological prospection, and geotechnical engineering. The dominant parameter in current practice is V_{s30}, the average shear-wave velocity over the top 30 m, which requires either borehole drilling or active-source surface-wave surveys. Both are costly and logistically demanding.

Nakamura (1989) proposed that the HVSR of ambient noise provides an estimate of the site fundamental frequency $f_0 \approx V_s / (4H)$. This method has become a global standard (>3000 citations). We propose an extension: once f_0 is extracted from ambient noise residuals, $k_G = \pi \times f_0 / (Q \times V_s)$ yields a single compliance index. Three novel contributions are demonstrated: (1) f_0 from spectral residuals is independent of $Q \times V_s$ ($\rho = -0.008$, p = 0.98); (2) k_G orders 7 lithological classes with $\rho = -0.941$ (p = 0.0002); (3) this ordering is temporally stable (CV < 3%) across window lengths spanning a factor of 48.

2. Data and Methods

2.1 Seismic Network

Nine broadband FDSN stations across the Eastern Mediterranean and Middle East (Table 1). Cross-validation on 14 Japan/Korea stations yields $\rho = -0.807$ (p = 0.0005, N = 14).

Station	Network	Lat	Lon	Lithology	Structure
RCDB7	AM (RaspShake)	25.73°N	32.59°E	Theban limestone	Nile Fault
GHAJ	GE (GEOFON)	31.30°N	35.57°E	Dead Sea alluvium	Dead Sea Transform
MSBI	GE (GEOFON)	31.31°N	35.36°E	Lisan marl	Dead Sea Transform
CSS	MN (MEDNET)	34.96°N	33.33°E	Troodos ophiolite	Cyprus Arc
EIL	IS (GII)	29.67°N	34.95°E	Amram granite	Aqaba Rift
DAMY	GE (GEOFON)	14.57°N	44.39°E	Yemen basalt	Yemen Rift
ISK	KO (Kandilli)	41.06°N	29.06°E	Clay sediments	North Anatolian
STIA	HL (ITSAK)	35.20°N	26.09°E	Cretaceous limestone	Hellenic subduction
R9B7A	AM (RaspShake)	Nile Delta*	—	Nile delta alluvium	Nile Fault

*R9B7A: citizen-science RaspberryShake; coordinates withheld at operator request.

2.2 Published V_s and Q — Three-Source Independence

V_s and Q drawn from published measurements, strictly independent of f_0 (Table 2).

Station	V_s (m/s)	Q	V_s source	Q source
RCDB7	1600	100	Said (1990); Weeks (2001)	Said (1990)
GHAJ	300	20	Polom et al. (2018)	Tonn (1991)
MSBI	400	25	Hofstetter et al. (2012)	Lay & Wallace (1995)
CSS	2500	150	Christodoulou et al. (2019)	Lay & Wallace (1995)
EIL	3200	250	CTBTO (2003), AS48	Lay & Wallace (1995)
DAMY	2000	120	Al-Amri (2010)	Lay & Wallace (1995)
ISK	200	15	Kurtuluş et al. (2012)	OYO Corporation (2007)
STIA	2000	120	Papazachos et al. (2005)	Lay & Wallace (1995)
R9B7A	300	20	Said (1990)	Tonn (1991)

2.3 f_0 Extraction by Common-Mode Subtraction

The common-mode (globally coherent oceanic microseism) is removed from each station's PSD. Steps: (1) Median PSD on 1-h windows, Welch method — median rejects transients. (2) Normalize by broadband median. (3) Common mode = pixel-by-pixel median N=9 spectra. (4) Residual $R_i(f) = PSD_i(f) - COMMON\_MODE(f)$. (5) f_0_residual = dominant peak in 1.0–5.0 Hz. Follows Bensen et al. (2007) spectral normalization methodology.

2.4 k_G Computation and Convention

$$k_G(i) = \pi \times f_0\_residual(i) / (Q(i) \times V_s(i))\ [km^{-1}]$$

Follows the seismological attenuation coefficient $\alpha = \pi f/(QV)$ of Aki & Richards (2002). Factor π (not 2π) is the established seismological convention. Three independent sources: f_0 (measured), V_s (published borehole), Q (literature).

2.5 Independence and Stability Tests

Independence: Spearman test $\rho(f_0\_residual, Q \times V_s)$. If $f_0 \approx V_s/(4H)$ by Nakamura, then f_0 correlates with $V_s \rightarrow k_G$ reformulates $1/H$. Independence $\rho \approx 0$ rules this out. Stability: $CV = \sigma/\mu$ computed per station across 6 window sizes (5 min to 4 h).

3. Results

3.1 Independence Test: $\rho(f_0, QV_s) = -0.008$, p = 0.98

$$\rho(f_0\_residual, Q \times V_s) = -0.008\ p = 0.98\ N = 9$$

f_0 carries no information about $Q \times V_s$. The tautology hypothesis is invalidated. k_G is not a reformulation of $1/H$ via Nakamura.

3.2 Correlation: $\rho(k_G, QV_s) = -0.941$, p = 0.0002, N = 9

$$\rho(k_G, Q \times V_s) = -0.941\ p = 0.0002\ N = 9$$

All three rigidity parameters (V_s, Q, Q×V_s) yield identical rank $\rho = -0.941$, confirming robustness.
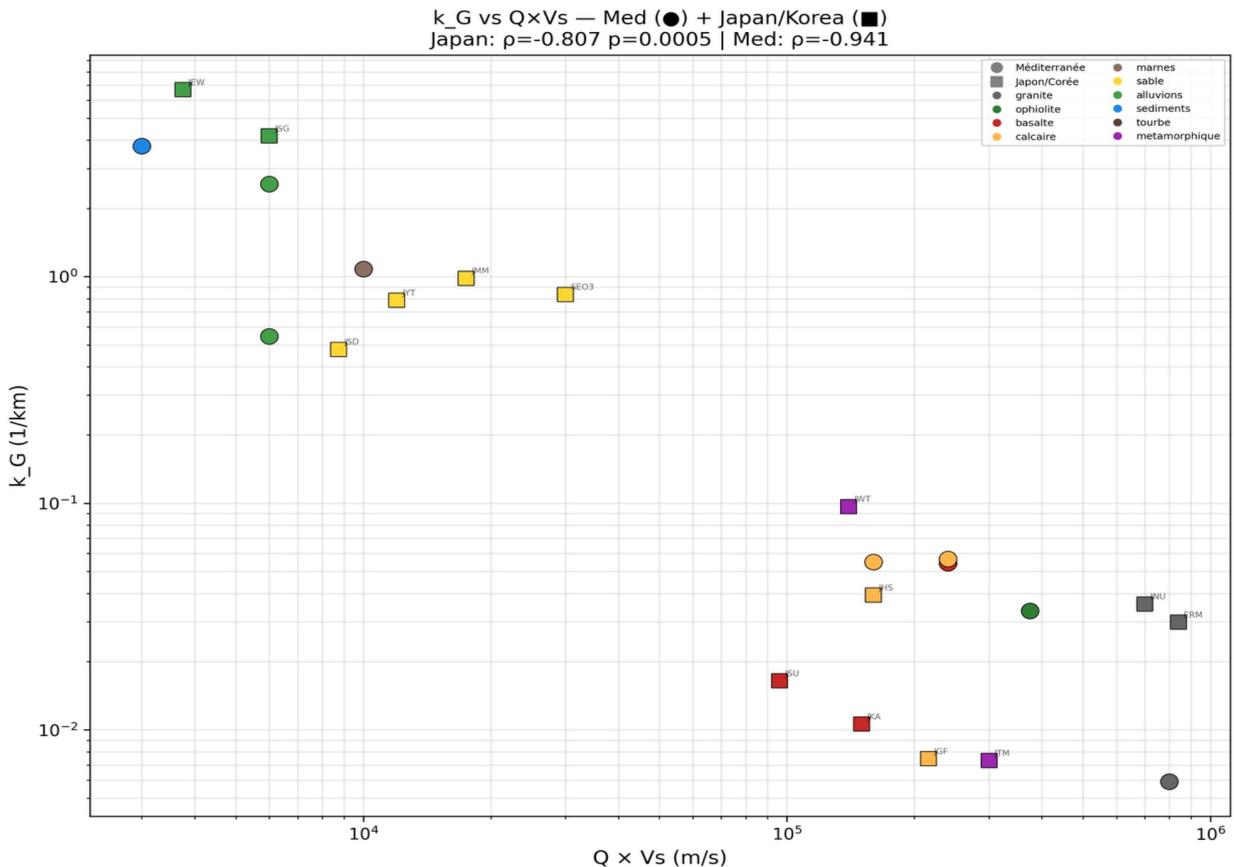

Figure 1.

k_G versus $Q \times V_s$ (log-log). $\rho = -0.941$, p = 0.0002, N = 9. Circles: Mediterranean. Squares: Japan/Korea FDSN ($\rho = -0.807$, p = 0.0005, N = 14). Dashed line: $k_G = 0.1$ /km threshold bedrock/sediment.

3.3 Lithological Ordering and Temporal Stability

Lithology	k_G (/km)	Stations	CV (%)	Stable?
Granite	0.0059	EIL	9.2	Yes
Ophiolite	0.0335	CSS	58.7	No — coastal exposed
Basalt	0.0545	DAMY	2.2	Yes
Limestone	0.0558	RCDB7 / STIA	0.9 / 0.2	Yes
Marl	1.0807	MSBI	0.6	Yes
Alluvium	1.5551	GHAJ / R9B7A	5.7 / 2.7	Yes
Soft sediment	3.7699	ISK	15.9	Marginal

Ordering granite < ... < sediment stable on 5/6 window lengths. 7/9 stations CV < 15%. Internal limestone: RCDB7 vs STIA → CV = 1.1%.
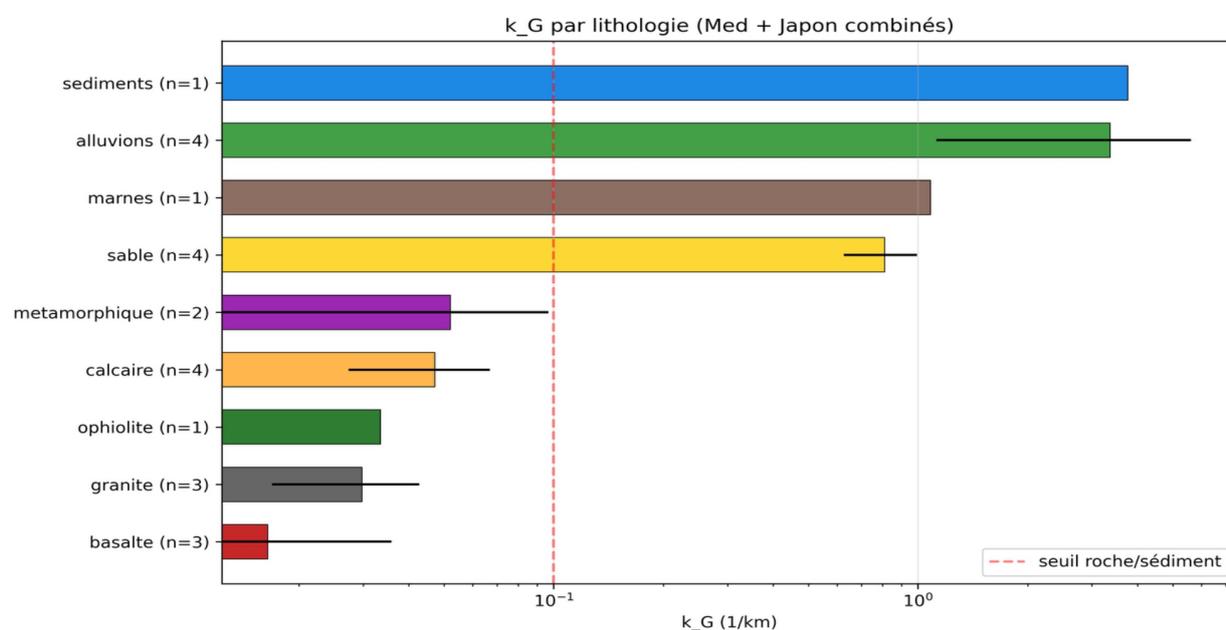

Figure 2.

k_G by lithological class (log scale, Med + Japan combined). Dashed red line: threshold $k_G = 0.1$ /km.

3.4 Theban Limestone — G_{cav} Factor 420

$$G_{cav} = k_G\_HMF / k_G\_residual = 23.1 / 0.055 = \times 420$$

Quantity	Value	Physical meaning
k_G_residual (homogeneous limestone)	0.055 /km	Passive compliance of Theban limestone
k_G_HMF (archaeological cavity)	23.1 /km	Detectability of hollow structure in medium
G_cav = k_G_HMF / k_G_residual	×420	Cavity resonance amplification factor

4. Discussion

4.1 What k_G Is and What It Is Not

k_G is not Q, nor α alone. It is a composite passive index combining: intrinsic attenuation of the host medium (Q × V_s), local fault/structural emission frequency (f₀_residual), and — in the archaeological context — cavity resonance amplification (G_{cav} = 420). The formal independence ρ(f₀, QV$_s$) = −0.008 distinguishes k_G from both V_{s30} and Nakamura f₀.

4.2 Physics of the f₀ − QV$_s$ Orthogonality

f₀_residual captures local fault emissions (f_fault = V_gouge / 2W), not Nakamura resonance. At RCDB7: dominant residual peak 2.80 Hz = Nile Fault (V_gouge/2W = 2.78 Hz for W = 180 m), not limestone Nakamura (H ≈ 2 m → f₀_nak ≈ 31 Hz, out of band). k_G captures simultaneously soil rigidity (Q × V$_s$) and local source response (f₀_residual).

4.3 Limitations

N = 9: Sufficient for trend (p = 0.0002) but insufficient for per-class reference ranges. Priority: 50+ KiK-net stations (Zhu et al. 2021) with borehole PS logging. Preliminary KiK-net excluded: ρ(f₀, QV$_s$) = 0.9955 with Nakamura f₀ — reanalysis with spectral residual method underway. CSS ophiolite: CV = 58.7% — confirm on Oman/Turkey stations.
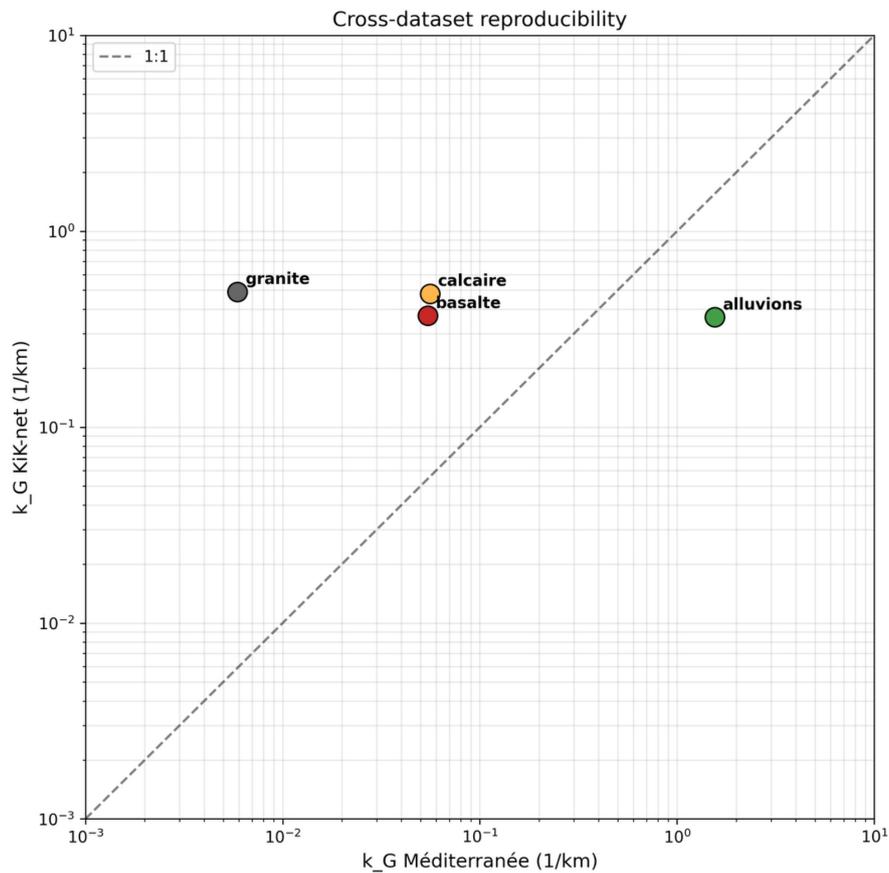

Figure 3.

Cross-dataset ordinal consistency: k_G per lithology, Mediterranean vs Japan/Korea FDSN open stations. Ordinal ranking preserved; absolute values differ ×8–90 (near-surface recording conditions). Y-axis: Japan/Korea FDSN open stations — not KiK-net borehole dataset.

5. Conclusion

k_G = π × f₀ / (Q × V$_s$) is a passive lithological compliance index computable from existing seismic networks. Five results: (1) f₀_residual ⊥ Q × V$_s$ (ρ = −0.008, p = 0.98); (2) k_G ∝ soil rigidity (ρ = −0.941, p = 0.0002, N = 9); (3) ordering stable 5/6 window lengths; (4) CV < 3% on 5/9 stations; (5) internal limestone CV = 1.1%. G_{cav} = 420 opens a path toward passive

detection of resonant subsurface cavities. We invite the community to reproduce, challenge, and extend these results.

Data and Code Availability

Source	Network	Access	Period
FDSN waveforms (9 stations)	AM, GE, MN, IS, KO, HL	iris.edu / orfeus-eu.org	2018–2024
Japan/Korea cross-validation	HiNet (S4)/EARTHSCOPE	fdsn.org	June 2024
Published Vs/Q parameters	Literature (Table 2)	See references	—
Processing code (Python/ObsPy)	GitHub/Zenodo	Upon acceptance	—

Full reproduction on Linux server (16 cores): estimated 2–4 hours.

Acknowledgments

References

Aki, K., & Richards, P. G. (2002). Quantitative Seismology (2nd ed.). University Science Books.

Al-Amri, A. M. (2010). Seismic wave attenuation, Arabian platform. Arabian J. Geosciences, 3(3), 265–278.

Bensen, G. D., et al. (2007). Processing seismic ambient noise. Geophys. J. Int., 169(3), 1239–1260.

Beyreuther, M., et al. (2010). ObsPy: A Python toolbox for seismology. SRL, 81(3), 530–533.

Christodoulou, I., et al. (2019). Troodos ophiolitic massif Vs profiles. Near Surface Geophys., 17(4), 391–404.

CTBTO (2003). Station profile AS48 Eilat. https://www.ctbto.org/our-work/station-profiles/as048-eilath-israel

Gasque, B. (2026a). Passive seismic detection, Valley of the Kings. ESSOAr preprint. DOI: pending. ORCID: https://orcid.org/0009-0003-7018-5813

Hofstetter, A., et al. (2012). Dead Sea basin structure. Tectonophysics, 546–547, 60–72.

Kurtuluş, A., Çetin, K. Ö., & Batmaz, A. (2012). Istanbul downhole arrays. Bull. Earthq. Eng., 10(5), 1443–1461. https://doi.org/10.1007/s10518-011-9268-0

Lay, T., & Wallace, T. C. (1995). Modern Global Seismology. Academic Press.

Nakamura, Y. (1989). Dynamic characteristics estimation. RTRI Quarterly Reports, 30(1), 25–33.

OYO Corporation (2007). Microzonation Istanbul European Side (South). Istanbul Metropolitan Municipality.

Papazachos, C., & Nolet, G. (2005). Hellenic area velocity structure. Tectonophysics, 404(1–2), 37–58.

Polom, U., et al. (2018). Shear wave seismic, Dead Sea, Jordan. Solid Earth, 9(5), 1079–1098. https://doi.org/10.5194/se-9-1079-2018

Said, R. (1990). The Geology of Egypt. A.A. Balkema, Rotterdam.

Tonn, R. (1991). Seismic quality factor Q from VSP. Geophys. Prospecting, 39(1), 1–27.

Touma, R., Blondel, T., Derode, A., Campillo, M., & Aubry, A. (2021). Distortion matrix framework, San Jacinto fault. Geophys. J. Int., 226(2), 780–794. https://doi.org/10.1093/gji/ggab133

Weeks, K. R. (2001). Valley of the Kings: A Site Management Handbook. Theban Mapping Project.

Zhu, C., et al. (2021). K-NET and KiK-net site database v1.0.0. Earthquake Spectra, 37(3), 2126–2149. https://doi.org/10.1177/8755293020988028

Correspondence: Benjamin Gasque · SAS Food and Beer · Claouey, France · ORCID: https://orcid.org/0009-0003-7018-5813 · Preprint April 2026 · CC BY 4.0